Molecular Crystals and Liquid Crystals
Publication details, including instructions for authors and subscription information:
http://www.tandfonline.com/loi/gmcl16

Solved and Unsolved Problems in the Solid-State Polymerization of Diacetylenes

V. Enkelmann [a], G. Wenz [a], M. A. Müller [a], M. Schmidt [a] & G. Wegner [a]
[a] Institut für Makromolekulare Chemie, Universität Freiburg, Stefan-Meier-Str. 31, D-7800, Freiburg
Version of record first published: 17 Oct 2011.

To cite this article: V. Enkelmann , G. Wenz , M. A. Müller , M. Schmidt & G. Wegner (1984): Solved and Unsolved Problems in the Solid-State Polymerization of Diacetylenes, Molecular Crystals and Liquid Crystals, 105:1, 11-39

To link to this article: http://dx.doi.org/10.1080/00268948408071640

Mol. Cryst. Liq. Cryst. 1984, Vol. 105, pp. 11-39
0026-8941/84/1054-0011/$18.50/0

Printed in the United States of America

SOLVED AND UNSOLVED PROBLEMS IN THE SOLID-STATE POLYMERIZATION OF DIACETYLENES

V. ENKELMANN, G. WENZ, M.A. MÜLLER, M. SCHMIDT, G. WEGNER
Institut für Makromolekulare Chemie, Universität Freiburg, Stefan-Meier-Str. 31, D-7800 Freiburg

Abstract Knowledge of the conversion dependence of the molecular weight and molecular weight distribution is necessary in order to understand the mechanism of polymerizations. Until recently the determination of molecular weights has been an unsolved problem in the area of the solid-state polymerization of diacetylenes. In this paper a survey is given of experiments on the solution properties of two soluble polydiacetylenes. The polydiacetylene chain behaves in solution like a random coil of worm-like chains with typical persistence length of 150 Å. The yellow-to-blue transition in P3BCMU was found to be connected to an aggregation process.

Since the first description of the solid-state reactivity of some diacetylene intermediates in the indigo synthesis [1] the topochemical polymerization of diacetylenes has developed to one of the best investigated polymerization reactions. However, many details of this unique reaction are not fully understood to date. In this paper some recent approaches to

solve some of the open questions will be reviewed.
In many cases the solid-state polymerization of diacetylenes proceeds as an ideal homogeneous topochemical reaction. The polymer chain is formed by a 1,4 addition reaction of monomer units which are arranged in a stack. The growing macromolecules form a solid solution in the monomer matrix and in many cases the monomer crystal is gradually transformed into the defect-free macroscopic polymer crystal. The packing of the diacetylene monomers can be characterized by the stacking distance d and by the angle ϕ between the stacking axis and the reactive triple bond system (Fig. 1).

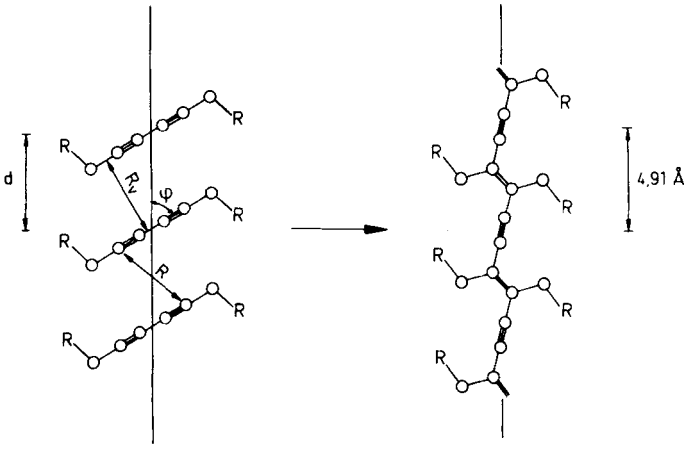

FIGURE 1 Schematic representation of the packing of diacetylene monomers and the topochemical polymerization (R_v : van der Waals distance).

In a first approximation it can be assumed that during the reaction the substituents R retain their position while the

diacetylene groups rotate in order to bring the reacting C atoms in close contact. Using simple geometrical considerations it can be predicted that maximum reactivity will be observed for the packing parameters $d \simeq 5$ Å and $\phi \simeq 45^{\circ}$. This is shown in Fig. 2 where the parameters of diacetylene monomers obtained in crystal structure analyses are summarized [2-6].

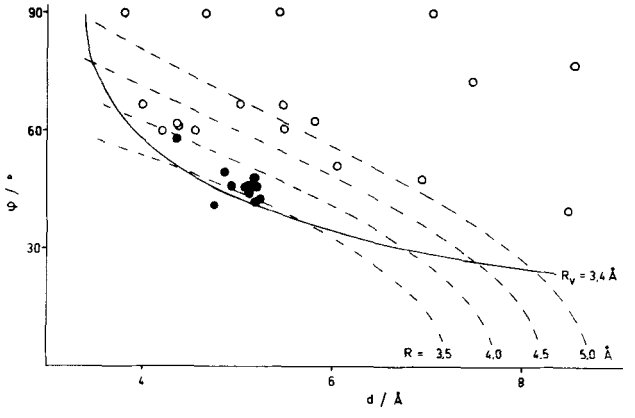

FIGURE 2 Plot of d vs ϕ . The broken lines are lines of constant distance R between the reacting atoms. Open points: inactive structures, closed points: reactive structures.

High reactivity is only observed if the separation R between the reacting atoms is less than 4 Å. A similar requirement is also observed in other solid-state reactions, e.g. the 2 + 2 cycloaddition of olefins [7].

However, it should be noted that there is no obvious correlation between the absolute reactivity or the reaction kinetics and the packing parameters. In some cases the reactivity of monomers with identical packing and isomorphous

crystal structures, e.g. PTS, R = $-CH_2O-SO_2-C_6H_4-CH_3$ and PFBS, R = $-CH_2O-SO_2-C_6H_4-F$, differs by a factor of 10 or more [8].

Although much is known about the reaction kinetics and the reactive intermediates involved in the reaction [9-21] there is no theory which is able to predict the reaction rate without adjustable parameters [22]. One of the reasons for this failure are rather complex side group motions and energy transport processes during the reactiong which cannot be taken into account by the existing theories [5,6,23].

Far more insight into the polymerization mechanism than the overall reaction rate gives the conversion dependence of the molecular weight and its distribution. Owing to the extreme insolubility of most of the better investigated PDAs, however, only very limited experimental data have been available until recently [24-27]. Since Patel detected in 1978 that poly(4,6-decadiin-1,10-diol-bis(n-butoxycarbonylmethylurethane)), P3BCMU is a readily soluble polymer [28-30] the study of the solution properties of PDA chains attracted increasing interest. More recently a fair amount of soluble PDAs have been synthesized in several laboratories [31-33]. In the following the polymerization and the solution properties of two better investigated examples, PTS-12 (R =$-(CH_2)_4-OSO_2-C_6H_4-CH_3$) and 3BCMU (R = $-(CH_2)_3-OCONH-CH_2COO-(CH_2)_3-CH_3$) will be reviewed.

THE MONOMERS

The dosage conversion curve for the polymerization of PTS-12 with ^{60}Co γ-radiation is shown in Fig. 3. The polymerization is characterized by an induction period which is followed by a rapid reaction. For complete conversion a dosage of 15 Mrad is required. The onset of the rapid reaction is connected

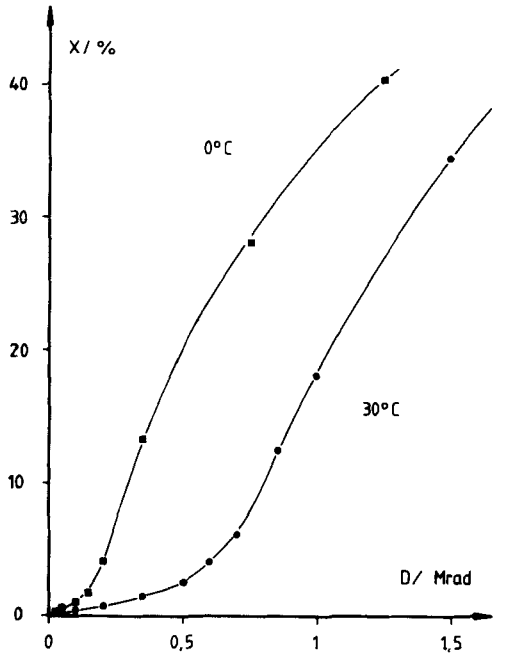

FIGURE 3 Dosage conversion curves for the polymerization of PTS-12 at $0^{\circ}C$ and $30^{\circ}C$.

with a phase transition [34]. In the monomer structure the b axis is doubled. The transition can be followed by a continuous decrease of the intensities of all reflections having odd k indices. The dependence of the lattice parameters determined at 110 K on the conversion is shown in Fig 4. The doubling of the unit cell in the monomer phase is explained by the fact that contrary to the polymer chain the monomer unit is not centrosymmetric. A projection of the monomer and polymer crystal structures on a common plane is shown in Fig. 5. Polymerization proceeds in the c direction. Neighboring monomer units are separated by 5.19 Å making an angle of

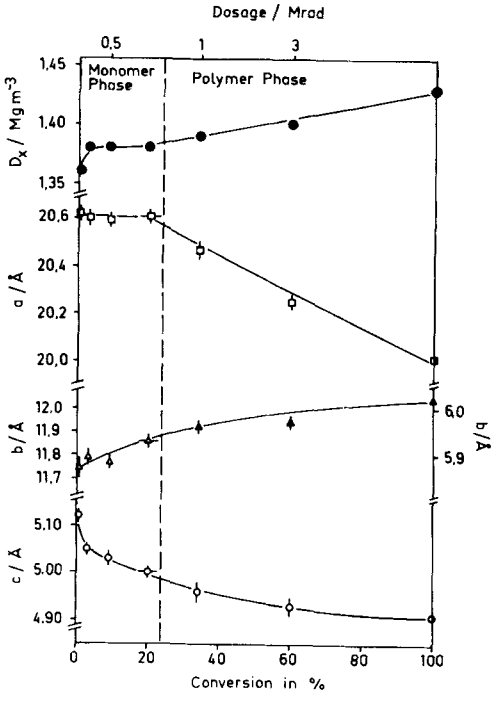

FIGURE 4 Dependence of the lattice parameters of PTS-12 on the conversion.

47.9° with c. These packing parameters are well within the range where high reactivity is expected. It can be seen in Fig. 5 that the monomer has two differently oriented side groups. The centers of the triple bond systems are separated from the symmetry centers of the polymer chain by about 1 Å, i.e. the polymerization is accompanied by unusually large translational and rotational motions without any destruction of the crystal. The rather complex motions in PTS-12 can be regarded as a special case of those observed in other diacetylenes. Here the whole methylene spacer group is in-

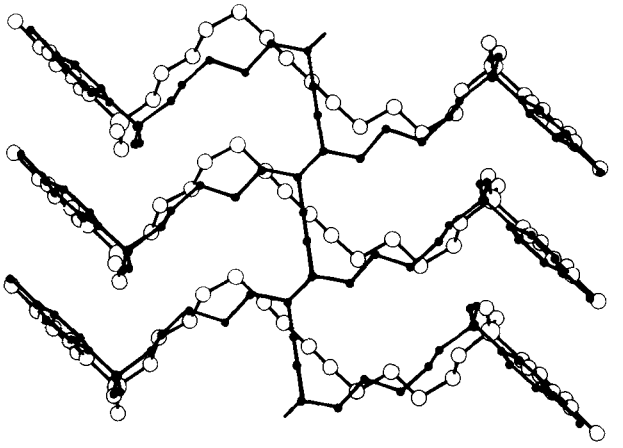

FIGURE 5 Projection of the monomer and polymer crystal structures of PTS-12 on a common plane.

cluded in the conformational changes necessary to bring the reacting C atoms in close contact. The terminal p-toluene-sulfonate groups are already in the monomer pseudo-centro-symmetrically related (cf. Fig. 5) and retain their position.

3BCMU cannot be quantitatively polymerized by γ-irradiation. After a high initial polymerization rate the reaction slows down and a limiting conversion of approximately 65 percent is reached at high dosages.

The crystal structure of the monomer was determined at 110 K using standard techniques [6]. Pertinent crystallographic data and details of the structure analysis are given in Table 1. Final atomic parameters are summarized in Table 2 †.

† Tables of parameters of the H atoms, observed bond lengths and angles and of observed and calculated structure factors are available upon request from V. Enkelmann.

TABLE 1 Crystallographic data and details of the crystal structure determination for 3BCMU monomer. E.s.d.'s are given in parentheses.

a / Å	58.80(2)
b / Å	4.90(1)
c / Å	8.69(1)
β / °	99.0(3)
space group	C2/c
D_x / gcm^{-3}	1.28
measured unique reflections	942
observed reflections	832
final R index	0.065

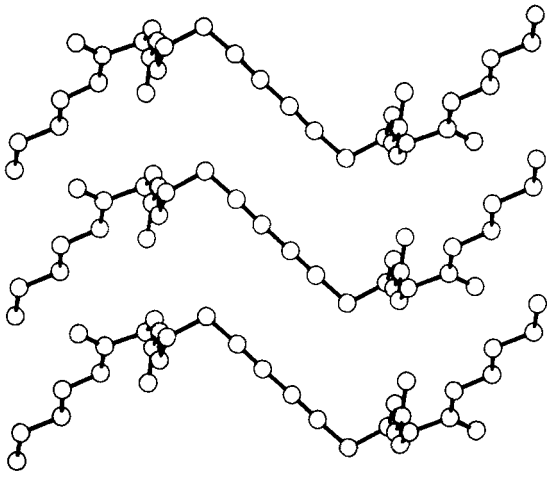

FIGURE 6 Projection of the crystal structure of 3BCMU monomer on the plane of the diacetylene stack.

TABLE 2 Final atomic parameters for 3BCMU monomer. The values given are fractional coordinates ($x10^4$) and isotropic temperature factors. E.s.d.'s are given in parentheses.

atom	x	y	z	$B/\AA^2$
C1	4932(1)	4074(18)	5287(7)	1.54(12)
C2	4819(1)	2350(17)	5824(7)	1.20(12)
C3	4684(1)	423(18)	6525(7)	1.81(13)
C4	4499(1)	1827(18)	7309(7)	1.70(13)
C5	4322(1)	3400(19)	6225(7)	2.07(14)
O1	4199(1)	1441(12)	5162(5)	1.66(9)
C6	4029(1)	2543(21)	4094(8)	1.93(15)
O2	3987(1)	4987(14)	4037(6)	2.30(11)
N1	3933(1)	599(14)	3157(6)	1.48(10)
C7	3736(1)	1445(18)	1997(7)	1.80(13)
C8	3535(1)	2414(18)	2732(7)	1.58(13)
O3	3489(1)	1535(12)	3920(5)	2.31(10)
O4	3410(1)	4281(11)	1894(5)	1.65(9)
C9	3218(1)	5413(18)	2564(7)	1.89(14)
C10	3076(1)	7241(18)	1411(8)	2.00(14)
C11	2869(1)	8354(19)	2091(7)	1.74(13)
C12	2716(1)	10285(19)	1010(8)	2.53(15)

A projection of the crystal structure on the plane of the diacetylene stack is shown in Fig. 6. The packing parameters $d = 4.90\ \AA$ and $\phi = 47.3^\circ$ agree well with the observed high initial reactivity. The hydrogen bonds of the urethane groups are oriented along the stacking direction. No unusual

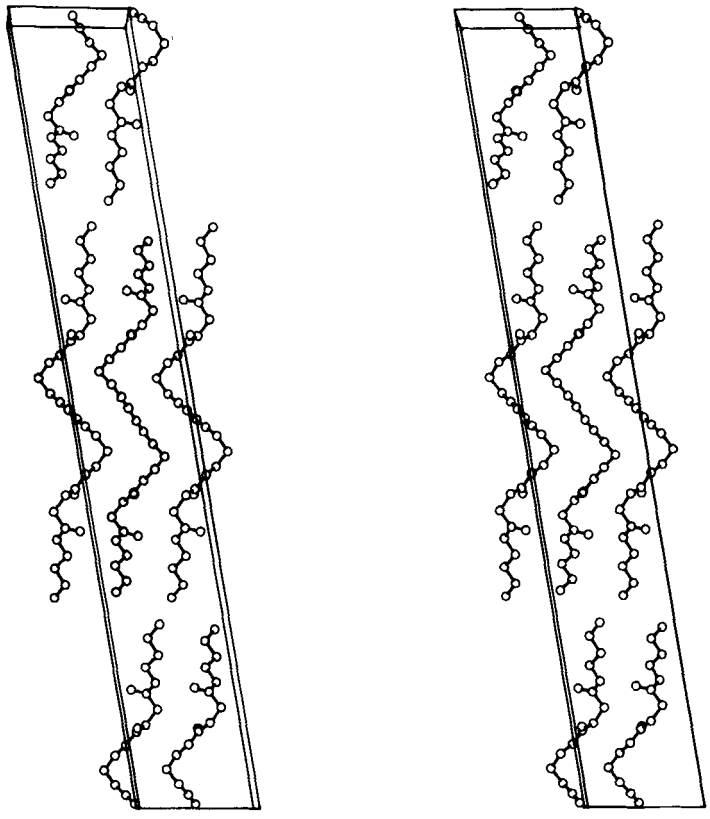

FIGURE 7 Stereoscopic view of the packing in 3BCMU. a is vertical and c horizontal.

bond lengths and angles are observed. A stereoscopic view of the packing is shown in Fig. 7. The monomer stacks are arranged in a way that neighboring sheets rotate in opposite directions during the reaction. This is probably the reason for the limited reactivity despite of the favourable packing parameters. Similar observations have been made previously with the diacetylene monomer TCDU [19,23]. Here two modifications with virtually identical packing parameters can be

obtained one of which (TCDU-2) shows a similar limited reactivity. Here again neighboring stacks perform rotations in opposite directions during the polymerization.

THE GROWTH OF THE POLYMER IN THE MONOMER MATRIX

As mentioned before the details of a specific polymerization reaction cannot be understood without knowledge of the molecular weight and molecular weight distribution and their relationship with the conversion and other experimental details. The developement of the molecular weight of PTS-12 as determined by gel permeation chromatography with increasing conversion is shown in Fig. 8. In the induction period short chains with an average degree of polymerization P_n = 60 are formed. At higher conversions the maximum shifts rapidly to higher values. Three curves with maxima at P_n = 60, 200 and 800 can be fitted to the experimental chromatograms. This is evident for the intermediate conversion range (Fig. 8b). Above approximately 20 percent conversion only the high molecular weight product is formed.

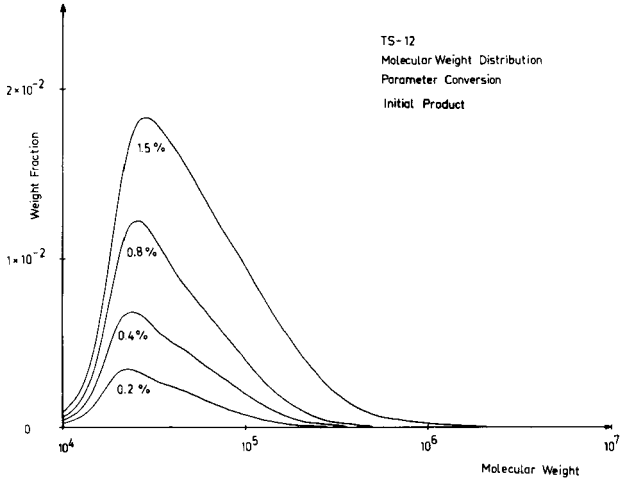

FIGURE 8a

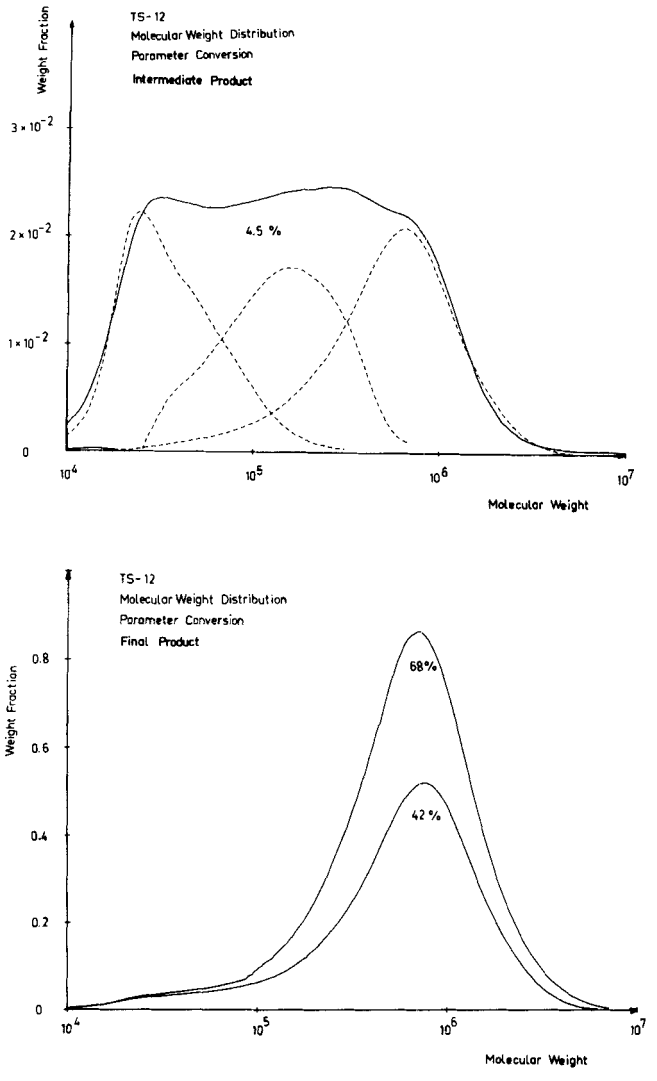

FIGURE 8 Molecular weight distribution of PTS-12 at three different stages of the polymerization.

Analysis of the data [31,35-37] shows that the chain initiation rate is constant over the entire conversion range with a rate constant $k_i = 6.25\ 10^{-4}$ Mrad^{-1} (G = 1.2 (100eV)$^{-1}$). Therefore the sudden increase of the overall reaction rate and the molecular weight must be attributed to an increase of the kinetic chain length. It is interesting to note that over the whole conversion range the short chains formed initially remain intact. This means that there is no re-initialization of "dead" chain ends and no combination of active and dead chain ends. As a consequence two different termination reactions must be considered. In the "free" termination an active chain end is desactivated by an until now unknown reaction. At higher conversions the "enforced" termination becomes more and more important. Here a growing chain is blocked by an already existing dead polymer in the same stack. In this kinetic model the kinetic chain length L is given by the ratio of the propagation and initiation rates. In Fig. 9 L is compared with the momentaneous degree of polymerization which can be independently determined from difference distributions. Within the experimental error both L and P_n show the same conversion dependence. The propagation rate is strongly temperature dependent. In Fig. 10 molecular weight distribution curves after irradiation with 0.05 Mrad at three different temperatures are shown. All distributions are bimodal with maxima at P_n = 60 and 400. At lower temperatures longer chains are formed. Since there is no gradual shift of the maximum it must be assumed that the chain grows by two different active chain ends the relative concentration of which is strongly temperature dependent. The chemical nature of the reactive chain ends cannot be deduced from our data.

However, spectroscopic studies of the reaction intermediates involved in the diacetylene polymerization have led to a similar reaction scheme as given below [15,16,19]:

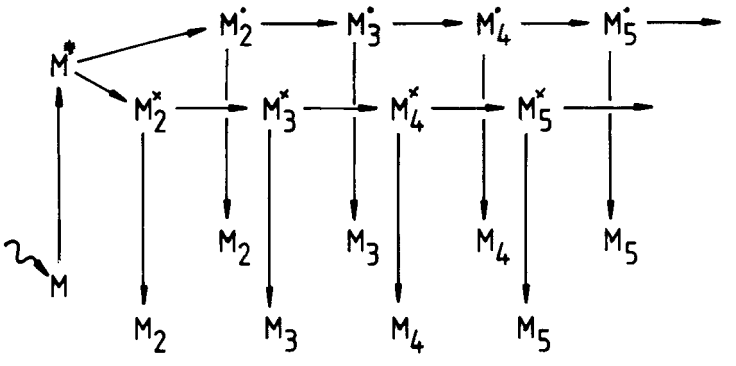

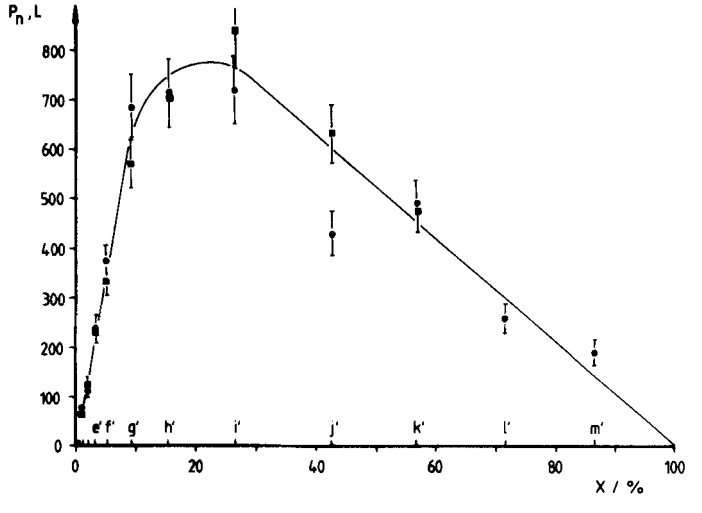

FIGURE 9 Comparison of the conversion dependence of the kinetic chain length L (●) and the momentaneous degree of polymerization P_n (■).

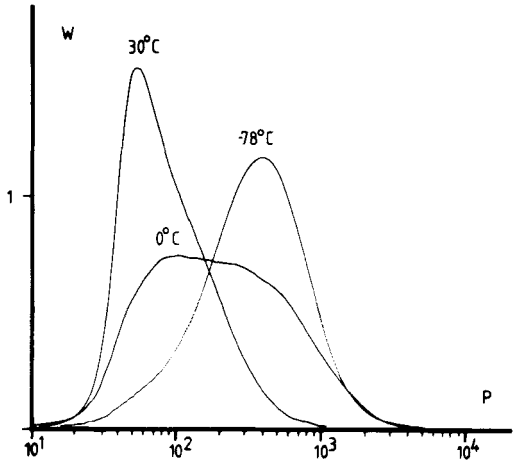

FIGURE 10 Temperature dependence of the molecular weight distribution of PTS-12 after irradiation with 0.05 Mrad.

THE SOLUTION PROPERTIES OF POLYDIACETYLENE CHAINS

The effective conjugation length

In Fig. 11 spectra of as polymerized crystalline PTS-12, the polymer dissolved in $CHCl_3$ and of the recrystallized, partially crystalline sample are shown in comparison. The strong blue shift of the absorption can be discussed in terms of a shortening of the effective conjugation length of the dissolved PDA chain. In the recrystallized sample two maxima are observed which can be assigned to the amorphous (A) and crystalline (K) parts. P_1 and P_o refer to the polymer formed in the initial (P_n = 60) and later stages (P_n = 800) of the polymerization.

Fig. 12 shows an assessment of the effective conjugation length according to the theory of Kuhn [38]. Here the optical

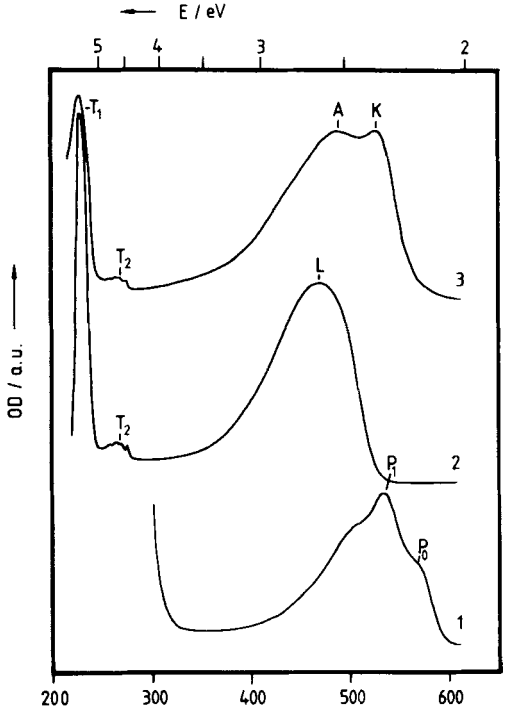

FIGURE 11 Transmission spectra of PTS-12. 1: Partially polymerized single crystal at 5 percent conversion, thickness 0.1 mm; 2: Solution in $CHCl_3$; 3: Recrystallized film, thickness < 10 µm.

bandgap E is plotted as a function of the number N of conjugated multiple bonds for PTS-12 and some model compounds. Using this empirical calibration curve an effective conjugation length N = 12, i.e. 6 monomer units can be determined for PTS-12 dissolved in $CHCl_3$. Similar values of the effective conjugation lengths of dissolved PDAs have been previously found by other authors [39] and also in our laboratory by

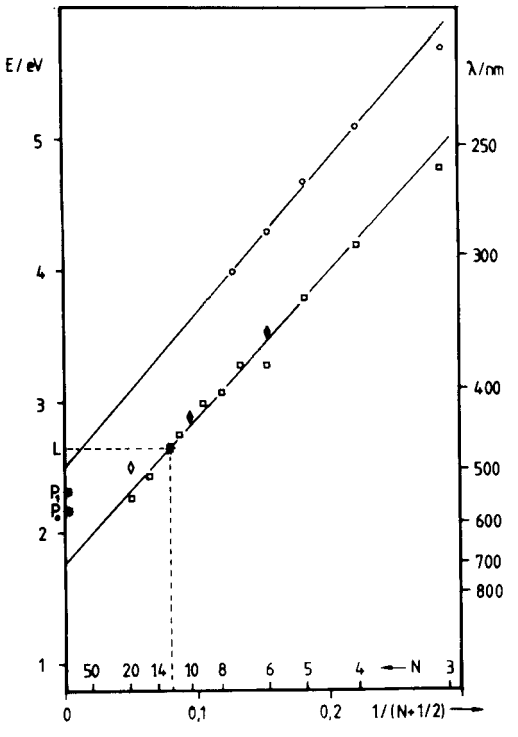

FIGURE 12 Dependence of the energy of the optical absorption of various polyconjugated compounds on the number N of multiple bonds [37]. ○ : Poly-ines, □ : trans polyenes, ◆ : polyen-ines, ◇ : oligomeric PTS-6.

other methods, e.g. ^{13}C NMR and resonant raman spectroscopy [36,37].

THE SHAPE OF THE DISSOLVED PDA CHAINS

The Zimm diagram obtained from light scattering experiments for PTS-12 (59 % conversion) dissolved in dichloroethane

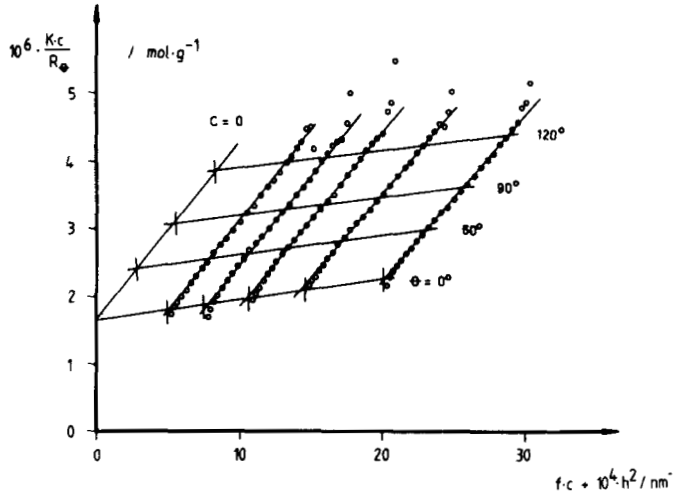

FIGURE 13 Zimm diagram of pristine PTS-12 (59 % conversion) dissolved in 1,2-dichloroethane, λ = 546 nm.

is shown in Fig. 13.

The angular dependence of Kc/R_θ gives information about the shape of the macromolecules in solution[40]. In Fig. 14 the reciprocal form factor $P_\theta^{-1} = M_w Kc/R_\theta$ is plotted as a function of $u^2 = \langle S^2 \rangle_z h^2$. The theory predicts for random coils a straight line with slope 1/3 (curve a)[40].

The two other downward bent curves in Fig. 14 (b,c) describe the behaviour of monodisperse and polydisperse rod-like molecules [41,42] with the same contour length. The experimental values also shown in Fig. 14 fit the theoretical behaviour of random coils excellently.

Pertinent data of the light scattering experiments for PTS-12 and P3BCMU are summarized in Table 3.

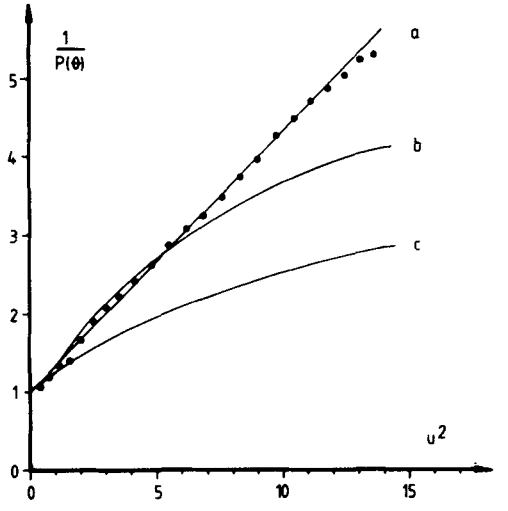

FIGURE 14 Plot of the reciprocal formfactor P_θ^{-1} vs. u^2 . a) random coils, b) monodisperse rigid rods, c) polydisperse rigid rods (M_w/M_n = 2).

TABLE 3 Results of the LS investigations of PTS-12 in 1,2-dichloroethane and P3BCMU in $CHCl_3$ [37].

Polymer	conversion %	λ/nm	M_w 10^{-3} $gmol^{-1}$	$\langle S^2 \rangle_z^{0.5}$ nm	A_2 $molcm^3g^{-2}$
PTS-12	59	546	630	70.8	$2.9\ 10^{-4}$
PTS-12	59	578	715	76.2	$4.1\ 10^{-4}$
PTS-12	90	546	1430	118	$2.0\ 10^{-4}$
P3BCMU	36	647	1360	94	$5.4\ 10^{-4}$

Further insight into the structure and properties of dissolved macromolecules are possible investigating the dependence of the radius of gyration on the molecular weight. Samples of different molecular weight of PDAs a readily obtained by photodegradation of solutions of the pristine polymers which are usually of very high molecular weight (cf. Table 3). The photodegradation is characterized by a random chain scission involving free radicals. It can be enhanced by addition of photolabile radical initiators and prevented by radical scavengers [43]. The dependence of the radius of gyration on M_w for several PTS-12 samples prepared by this technique is presented in Fig. 15.

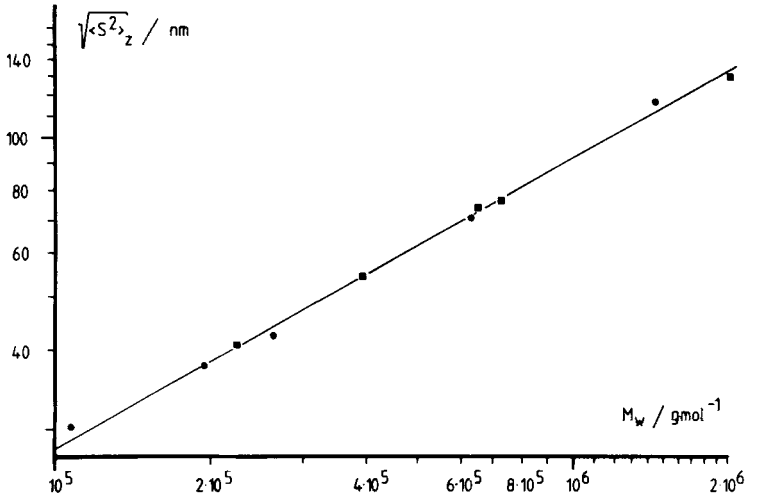

FIGURE 15 Dependence of the radius of gyration $\langle S^2 \rangle_z^{0.5}$ on M_w for PTS-12 dissolved in 1,2-dichloroethane. ● : λ = 546 nm, ■ : λ = 578 nm .

The experimental data shown in Fig. 15 can be expressed by

$$\langle s^2 \rangle_z^{0.5} = 0.45\, M_w^{0.55}$$

over a wide range of molecular weights. The exponent 0.55 is typical for coiled macromolecules in good solvents. For rigid rods an exponent of 1.0 is expected [40].

PTS-12, AN EXAMPLE FOR A WORM-LIKE CHAIN

The data collected on the solution behaviour of PDA chains can be readily discussed in terms of the worm-like chain (Porod-Kratky chain) [44,45]. In contrast to a Kuhn chain where perfect conjugated chain segments are separated by defects this concept for a chain molecule visualizes a continuous curvature of the chain skeleton, the direction of curvature at any point of the trajectory being random (Fig. 16). The stiffness of the chain is characterized by the average angle α between the directions of two consecutive segments. The persistence length ℓ_{pers} is then defined by

$$\ell_{pers} = 1/(1 - \langle \cos\alpha \rangle)$$

The light scattering data of PTS-12 solutions can be treated using the theories developed for worm-like chains. In Fig. 17 the characteristic ratio C_p of worm-like chains with a Schulz-Flory distribution ($M_w/M_n = 2$) is plotted as a function of the contour length for different values of the persistence length.

For small degrees of polymerization the theory predicts a strong initial increase of C_p which reaches a limiting value depending on ℓ_{pers}. This means that even a stiff chain assumes the properties of a random coil if it is

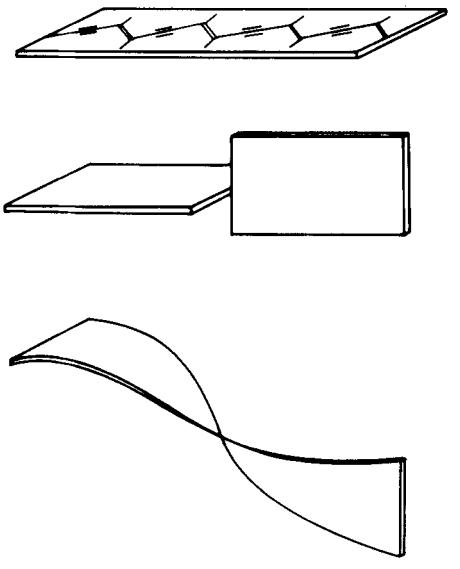

FIGURE 16 Schematic representation of the shape of PDA chains. Top: planar, fully conjugated chain; middle : Kuhn model; bottom: worm-like chain.

long enough. The experimental data for PTS-12 solutions fit the curve calculated for a worm-like chain with a persistence length of 40 units (190 Å) very well.

A similar treatment of the solution properties is shown in Fig. 18. Here the dependence of the Staudinger index $[\eta]$ on the molecular weight is plotted for different values of ℓ_{pers} [45,46]. The experimental values fit the curve calculated for a persistence length of 150 Å (31 units). The agreement between the viscosimetrically determined and ILS derived persistence length is reasonably good within the limits of approximations made in the calculations.

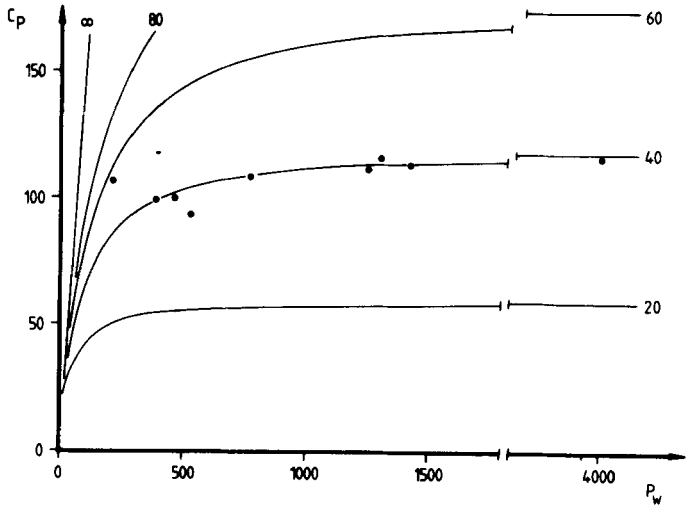

FIGURE 17 The dependence of the characteristic ratio C_p on the degree of polymerization P_w. The lines are calculated for worm-like chains with ℓ_{pers} in number of monomer units as parameter. ● : data from Fig. 15.

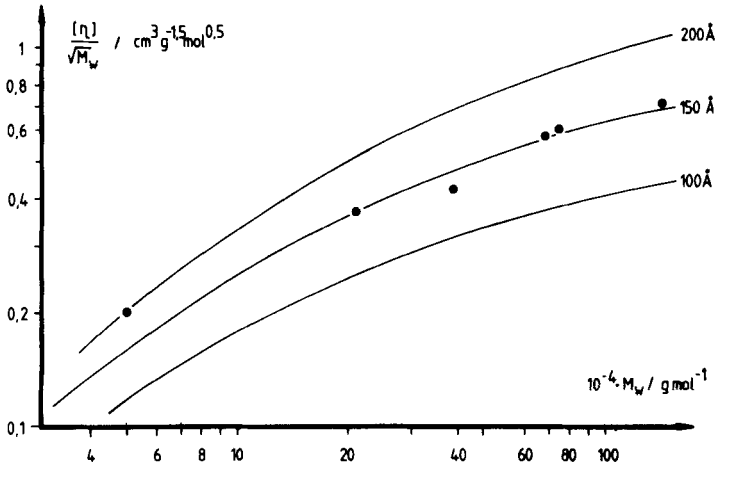

FIGURE 18 Molecular weight dependence of the Staudinger index $[\eta]$. The curves are calculated for the values of ℓ_{pers} given in Å.

Using the values found for the persistence length in this analysis an average angle $\alpha \approx 13^{\circ}$ can be calculated. This means that an average deformation of 3.3° per bond is necessary to produce the experimentally observed behaviour. It should be emphasized at this point that in this model the flexibility of the dissolved PDA chain is not brought about by defects, e.g. cis-double bonds which have been postulated by other authors[47,48]. All attempts to deliberately produce cis bonds failed and led to the chain scission described above.

THE YELLOW-TO-BLUE TRANSITION IN P3BCMU

P3BCMU and other polydiacetylenes with similar side groups have been noted to undergo dramatic colour changes when the solvent to non-solvent ratio or the temperature is changed[28-30,37,39,43]. This transition has been interpreted as a single chain coil-to-rod transition[28,30,47,48]. However, there is experimental evidence that this interesting phenomenon is connected to an aggregation process. Contrary to the yellow solution of P3BCMU ($M_w = 1.36\ 10^6$ $gmol^{-1}$) which can be filtered through a 0.5 μm millipore filter without any loss the polymer is completely removed filtering the equivalent blue solution through a 1.2 μm filter. The yellow-to-blue transition exhibits a rather peculiar time dependence. It is difficult to reach a true equilibrium state and the relative concentrations of the blue and yellow forms are not only time and temperature dependent but also on the history of the sample as it is commonly observed in nucleation controlled crystallization or aggregation phenomena.

The transition is accompanied by a dramatic increase in

light scattering intensity which has been interpreted quite controversally. Heeger et al.[47,48] explained this effect by an anomalous large refractive index increment whereas in our group it is attributed to the aggregation process already mentioned. More recently we have determined the refractive index increments of P3BCMU and P4BCMU in the yellow and blue states [49]. No anomaly in the refractive index increment in the blue solution could be detected.

It should be noted that the static and dynamic light scattering results were not reproducible quantitatively due to the fact that the properties of the blue "solution" are time dependent even after very long times. However, the analyses of the preliminary data lead despite of all experimental difficulties to the conclusion that in the blue state aggregates of 200 to 1000 chains are formed.

ACKNOWLEDGEMENT

This work was supported by the Stiftung Volkswagenwerk.

REFERENCES

1. A. Baeyer and L. Landsberg, Ber. dt. chem. Ges., 15, 61 (1884); A. Baeyer and L. Bloem, Ber. dt. chem. Ges., 17, 964 (1886).

2. R.H. Baughman, J. Polym. Sci., Polym. Phys. Ed., 12, 1511 (1974).

3. R.H. Baughman and K.C. Yee, J. Polym. Sci.,Macromol. Rev., 13, 219 (1978).

4. G. Wegner in Molecular Metals, ed. by W.E. Hatfield, Plenum Press, New York (1979) p. 209.

5. D. Bloor in Developments in Crystalline Polymers-1, ed. by D.C. Basset, Applied Science Publ., Barking (1982) p. 151.

6. V. Enkelmann, Adv. Polym. Sci., in preparation; V. Enkelmann, Habilitationsschrift, Freiburg (1983).

7. G.M.J. Schmidt, Solid State Photochemistry, Monographs in Modern Chemistry 8, Verlag Chemie, Weinheim (1976).

8. V. Enkelmann, Makromol. Chem., 184, 1945 (1983).

9. G.C. Stevens and D. Bloor, Chem. Phys. Lett.,40, 37 (1976).

10. R. Huber, M. Schwoerer, C. Bubeck and H. Sixl, Chem. Phys. Lett., 53, 35 (1978).

11. H. Sixl, W. Hersel and H.C. Wolf, Chem. Phys. Lett., 53, 39 (1978).

12. W. Hersel, H. Sixl and G. Wegner, Chem. Phys. Lett., 73, 288 (1980).

13. C. Bubeck, H. Sixl and W. Neumann, Chem. Phys., 48, 269 (1980).

14. H. Benk and H. Sixl, Mol. Phys., 42, 779 (1981).

15. H. Sixl, Adv. Polym. Sci., submitted.

16. H. Sixl, Proceedings of this Symposium.

17. H. Eichele, M. Schwoerer, R. Huber and D. Bloor, Chem. Phys. Lett., 42, 342 (1976).

18. H. Niederwald, H. Eichele and M. Schwoerer, Chem. Phys. Lett., 72, 242 (1980).

19. H. Gross, H. Sixl, C. Kröhnke and V. Enkelmann, Chem. Phys., 45, 15 (1980).

20. R.R. Chance, G.N. Patel, E.A. Turi and Y.P. Khanna, J. am. chem. Soc., 100, 1307 (1978).

21. Y. Hori and L.D. Kispert, J. am. chem. Soc., 101, 3173 (1979).

22. R.H. Baughman, J. Chem. Phys., 68, 3110 (1978).

23. V. Enkelmann, J. Chem. Res. (M), 3901 (1981).

24. G. Wegner, Z. Naturforsch. (b), 24, 824 (1969).

25. G. Wegner, J. Polym. Sci., Polym. Lett. Ed., 9, 133 (1971).

26. G. Wegner, Makromol. Chem., 145, 85 (1971).

27. V. Enkelmann, R.J. Leyrer and G. Wegner, Makromol. Chem., 180, 1787 (1979).

28. G.N. Patel, J. Polym. Sci., Polym. Lett. Ed., 16, 607 (1978).

29. G.N. Patel, R.R. Chance and J.D. Witt, J. Chem. Phys., 70, 4387 (1979).

30. G.N. Patel and E.K. Walsh, J. Polym. Sci., Polym. Lett. Ed., 17, 203 (1979).

31. G. Wenz and G. Wegner, Makromol. Chem., Rapid Commun., 3, 231 (1982).

32. C. Plachetta, N.O. Rau, A. Hauck and R.C. Schulz, Makromol. Chem., Rapid Commun., 3, 249 (1982).

33. C. Plachetta and R.C. Schulz, Makromol. Chem., Rapid Commun., 3, 815 (1982).

34. D. Siegel, H. Sixl, V. Enkelmann and G. Wenz, Chem. Phys., 72, 201 (1982).

35. G. Wenz and G. Wegner, Mol. Cryst. Liq. Cryst., 96, 99 (1983).

36. G. Wenz, Dissertation, Freiburg (1983).

37. G. Wenz, M.A. Müller, M. Schmidt and G. Wegner, Macromolecules, in press.

38. H. Kuhn, Fortschr. Chem. Org. Naturstoffe, 16, 169 (1958); 17, 404 (1959).

39 H.L. Shand, R.R. Chance , M. Le Postollec and M. Schott, Phys. Rev. B, 25, 4431 (1982).

40. W. Burchard in Applied Fibre Science Vol. 1, ed. by F. Happey, Academic Press, New York (1978) p. 381.

41. T. Neugebauer, Ann. Phys., 42, 509 (1943).

42 H. Goldstein, J. Chem. Phys., 21, 1255 (1953).

43 M.A. Müller and G. Wegner, Makromol. Chem., Rapid Commun., in press.

44 G. Porod, Monatsh. Chem., 80, 251 (1949); O. Kratky and G. Porod, Rec. Trav. Chim., 68, 1106 (1949).

45 P.J. Flory, Statistical Mechanics of Chain Molecules, Interscience Publ., New York (1949) p. 401.

46. H. Yamakawa and H. Fujii, Macromolecules, 7, 128 (1974).

47. K.C. Lim, L.A. Fincher and A.J. Heeger, Phys. Rev. Lett., 50, 1934 (1983).

48. A.J. Berlinsky, F. Wudl, K.C. Lim, C.R. Fincher and A.J. Heeger, Theory of the Rod-to-Coil Transition in Polydiacetylene, Preprint (1983); A.J. Heeger, Proceedings of this Symposium.

49. M.A. Müller, M. Schmidt and G. Wegner, Makromol. Chem., Rapid Commun., in press.